Polymers of Intrinsic Microporosity (PIMs)

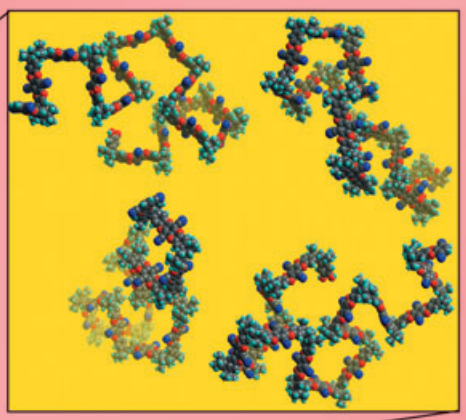

Solution

A rigid and contorted macromolecular structure provides solution-processable, organic microporous materials.

cast

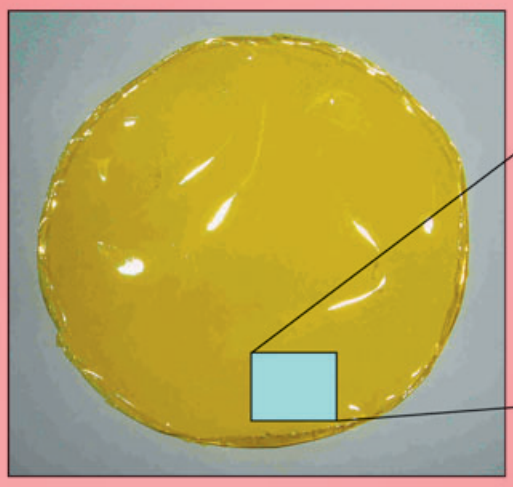

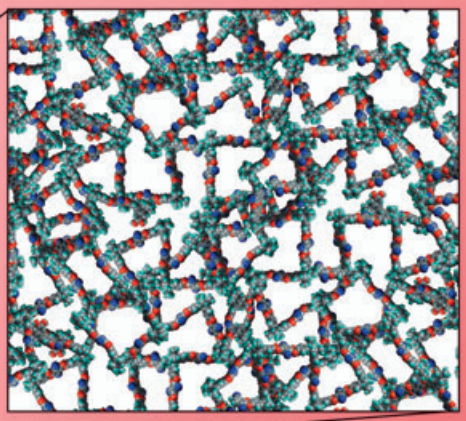

Microporous solid

Membranes for gas and chemical separations

DOI: 10.1002/chem.200400860 *Chem. Eur. J.* **2005**, *11*, 2610 – 2620

Polymers of Intrinsic Microporosity (PIMs): Bridging the Void between Microporous and Polymeric Materials

Neil B. McKeown,*[a] Peter M. Budd,[b] Kadhum J. Msayib,[b] Bader S. Ghanem,[b] Helen J. Kingston,[b] Carin E. Tattershall,[b] Saad Makhseed,[b] Kevin J. Reynolds,[b] and Detlev Fritsch[c]

Abstract: Novel types of microporous material are required for chemoselective adsorptions, separations and heterogeneous catalysis. This concept article describes recent research directed towards the synthesis of polymeric materials that possess microporosity that is intrinsic to their molecular structures. These polymers (PIMs) can exhibit analogous behaviour to that of conventional microporous materials, but, in addition, may be processed into convenient forms for use as membranes. The excellent performance of these membranes for gas separation and pervaporation illustrates the unique character of PIMs and suggests immediate technological applications.

Keywords: gas separation · membranes · microporous materials · phthalocyanines · polymers

Introduction

The study of materials that possess voids of molecular dimensions is an area of nanoscience with well-established technological applications.[1] Microporous materials are defined as solids that contain interconnected pores of less than 2 nm in size and consequently, they possess large and accessible surface areas—typically 300–1500 $m^2 g^{-1}$ as measured by gas adsorption. In the past decades, there has been an intense international effort to optimise conventional microporous materials, such as zeolites (aluminosilicates) and activated carbons, for specific applications in adsorption, separations and heterogeneous catalysis.[2–4] However, it is recognised that there is a pressing requirement to find entirely novel approaches to the synthesis of microporous materials to benefit fundamental research and to provide new technological opportunities.[3] In recent years there has been a growing emphasis on using organic components for the construction of microporous materials. It is anticipated that by careful selection of organic precursors it will be possible to exert precise control over the chemical nature of the accessible surface and to introduce specific molecular recognition or catalytic sites, thus facilitating chemoselective adsorption and the design of highly efficient heterogeneous catalysts.

Ordered crystalline structures have considerable visual impact, and none are more pleasing than those of the zeolites and related microporous solids. Therefore, it is understandable that the synthesis of "organic zeolites", in which rigid organic units are assembled into a microporous, crystalline structure by metal–ligand[5–7] or hydrogen bonds,[8] has developed into a major research area in the past decade. Initially, such materials were classified as "microporous" simply on the basis of X-ray crystal structures, even when the removal of solvent from the void space destroyed the crystalline order. Early examples also suffered from interpenetration of one lattice within the pores of another, resulting in restricted access to the internal void space. However, impressive advances based on coordination chemistry, especially by Yaghi and co-workers, have provided highly porous crystalline zeolite-like materials termed metal–organic frameworks (MOFs), which demonstrate vast accessible surface areas by the reversible adsorption of gas.[6,7] Recently, this methodology has been applied to the assembly of microporous structures by using porphyrin derivatives with catalytic potential.[9–12] It is also apparent that some co-

[a] Prof. N. B. McKeown
School of Chemistry, Cardiff University
PO Box 912, Cardiff, CF10 3TB (UK)
Fax: (+44) 29-2087-4030
E-mail: mckeownnb@cardiff.ac.uk

[b] Dr. P. M. Budd, Dr. K. J. Msayib, B. S. Ghanem, H. J. Kingston, Dr. C. E. Tattershall, Dr. S. Makhseed, K. J. Reynolds
School of Chemistry, University of Manchester
Manchester, M13 9PL (UK)

[c] Dr. D. Fritsch
Institute of Chemistry, GKSS Research Centre
Max-Planck-Strasse 1, 21502, Geesthacht (Germany)

 DOI: 10.1002/chem.200400860

ordination solids derived from more flexible organic ligands demonstrate dynamic behaviour with microvoids that can expand in the presence of an adsorbate.[5] Purely organic frameworks held together by hydrogen bonds are often too fragile to survive the removal of included solvent; however, some recently prepared hydrogen-bonded microporous materials, such as those reported from the groups of Wuest[8,13,14] and Aoyama,[15] show enhanced stability, but as yet, none have displayed high surface areas using gas adsorption.

The size- and shape-selectivity of adsorption derived from the well-defined micropores within crystalline solids, together with their aesthetic appeal, will ensure a continued interest in the synthesis of organic zeolite analogues. However, as demonstrated by various microporous inorganic materials (e.g., amorphous silica) and activated carbons, crystalline order is not a prerequisite for useful microporosity and this article will survey the less explored area of microporosity within amorphous organic materials, in particular network polymers and glass-forming polymers.

Activated carbon—the original organic microporous material: The ability of charcoal to adsorb contaminants from water has been known for thousands of years and today activated carbons are used in vast quantities as adsorbents, deodorizers and catalyst supports.[16,17] During the carbonisation process, planar graphene sheets are formed by the condensation of polynuclear aromatic units with the associated expulsion of side-chain groups. If suitable precursors are used, extended graphite sheets are produced that pack efficiently owing to the formation of an intermediate liquid-crystalline state, called the "carbonaceous mesophase", to give a nonporous solid. However during the carbonisation of coals and wood (commonly nutshells are employed), cross-linking occurs, which leads to extended graphitisation and ordered packing. The resulting network polymer, composed of randomly arranged graphene sheets, is intrinsically microporous.[16,17] Commercial carbons can offer surface areas well in excess of 1200 $m^2 g^{-1}$ depending upon the precursor material and post-carbonisation treatment. Given the method of preparation, it is unsurprising that most activated carbons possess a wide distribution of pore sizes ranging from microporous to mesoporous (20–50 nm) to macroporous (> 50 nm). Futhermore, the surface of activated carbons is chemically ill-defined with a large variety of oxygen- and nitrogen-containing functional groups present, in addition to the polycyclic aromatic units that form the graphene sheets.[18–21] The heterogeneous structure and chemical nature of the exposed surface area explains the ability of activated carbons to adsorb a wide range of organic compounds and metal ions, but limits its potential for chemo-selective processes.

Microporous Organic Network Polymers

It is clear from the activated carbons that non-crystalline organic materials may possess a microporous structure. In addition, there are examples of amorphous silica or metal oxide networks in which rigid organic subunits such as phenylene,[3] anthracene[22–24] or porphyrin[25] derivatives have been incorporated to give hybrid microporous materials. Despite the intense research effort concentrating on controlling polymer macro- and mesoporosity,[26–28] the concept of preparing purely organic microporous network polymers is almost entirely unexplored—with the exception of Webster's poly(arylcarbinol) networks, which demonstrated high surface areas (800–900 $m^2 g^{-1}$) by nitrogen adsorption.[29,30]

A few years ago, we initiated a research programme with the objective of preparing polymer networks with microporous structures similar to that of activated carbon, but with a range of well-defined surface chemistries. Considering its enormous commercial importance and the limited scope for systematic chemical or structural modification, it is surprising that the structure of activated carbon had not previously inspired imitation.

The general strategy involves the incorporation of extended aromatic components, to mimic the graphene sheets of activated carbons, within a rigid polymer network. Initially, the phthalocyanine macrocycle was selected as the aromatic component due to its extended planarity (diameter ~ 1.5 nm) and range of useful properties. These include oxidative catalysis if appropriate transition-metal ions are placed in its central cavity (e.g., the Merox process for the oxidative removal of sulfurous impurities in crude petrochemicals).[31] Previously prepared phthalocyanine network polymers show a strong tendency of the macrocycles to aggregate into columnar stacks, due to strong noncovalent interactions (primarily π–π interactions), resulting in nonporous solids.[32] Therefore, it was deemed essential to use a highly rigid and nonlinear linking group between the phthalocyanine subunits that would ensure their space-inefficient packing, thus preventing structural relaxation and consequent loss of microporosity. Perfectly suited to fulfil these requirements is a linking group derived from the commercially available 5,5′,6,6′-tetrahydroxy-3,3,3′,3′-tetramethyl-1,1′-spirobisindane (monomer **A1**). The spirocentre (i.e., a single tetrahedral carbon atom shared by two rings) of **A1** provides the nonlinear shape, and the fused-ring structure the required rigidity. Phthalocyanine network polymers are generally prepared from a bis(phthalonitrile) precursor through a cyclotetramerisation reaction that is usually facilitated by a metal-ion template. Such a reaction using the bis(phthalonitrile), prepared from the dioxane-forming reaction between monomer **A1** and 4,5-dichlorophthalonitrile, gives network polymers as free-flowing, highly coloured powders (Scheme 1). Spectroscopic (ESR, UV/visible absorption) and X-ray diffraction analyses of the network polymers confirm that the spirocyclic cross-links prevent a close packing of the phthalocyanine components, giving an amorphous microporous structure—as depicted by the model shown in

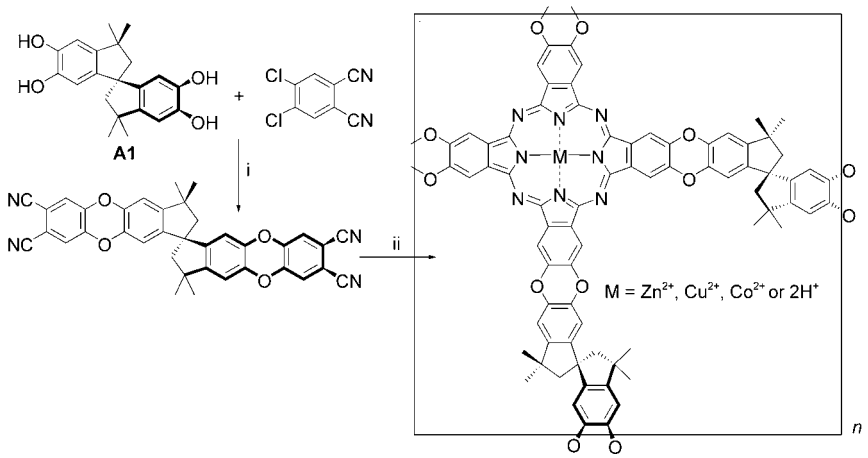

Scheme 1. The preparation of phthalocyanine-based microporous network polymers from spirocyclic monomer **A1**. Reagents and conditions: i) K_2CO_3, DMF, 80 °C; ii) metal salt, quinoline, 200 °C.

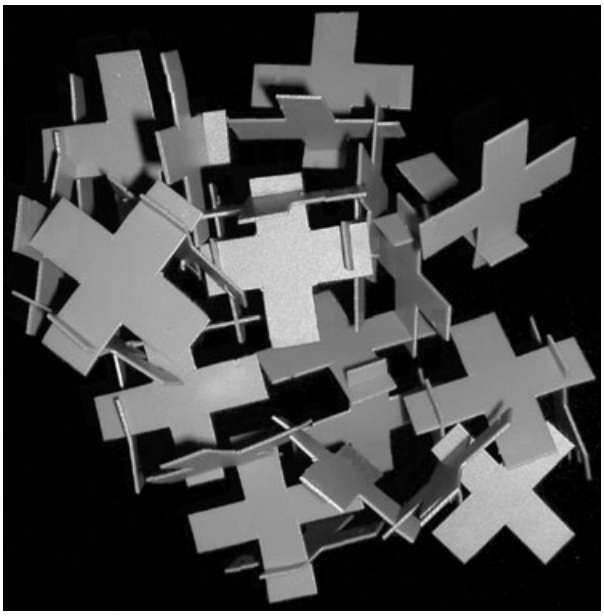

Figure 1. Simple three-dimensional model of the phthalocyanine-based microporous network polymer, with the aromatic macrocycles represented by cross-like shapes. The model helps to visualise the microporosity of the material, which is caused by the random and inefficient packing of the phthalocyanine units due to the rigid spirocyclic structure of the linking groups.

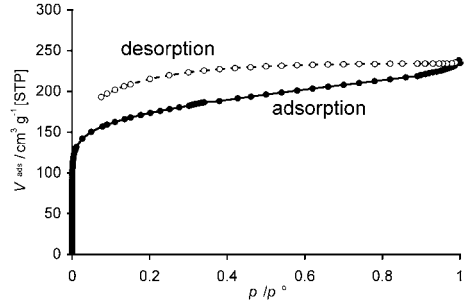

Figure 2. The nitrogen adsorption/desorption isotherm at 77 K for a microporous phthalocyanine network polymer (with $M = Co^{2+}$). The equivalent volume of adsorbed nitrogen at STP versus the relative pressure is plotted. From the isotherm a BET surface area of 650 $m^2 g^{-1}$ can be calculated. The shape of the isotherm and the large volume of nitrogen adsorbed at low relative pressure indicates microporosity.

Figure 1. Nitrogen adsorption measurements (e.g., Figure 2) show that the materials have high surface areas (in the range 500–1000 $m^2 g^{-1}$) with very significant adsorption at low relative pressure ($P/P^o < 0.01$) indicating microporosity.[33]

Following on from the successful preparation of these phthalocyanine network polymers of intrinsic microporosity (Network-PIMs), it was of interest to determine whether other rigid structures are also suitable components for use in the assembly of microporous organic materials. The related metal-containing porphyrins are an important family of catalysts, for example, iron–porphyrin derivatives can display similar activity to that of the cytochrome P450 enzymes, including the catalysis of alkene epoxidations and hydrocarbon hydroxylations.[34] These reactions are achieved by using environmentally benign oxidants, such as oxygen or hydrogen peroxide. Thus, the possibility of being useful heterogeneous catalysts makes porphyrins desirable components of a microporous material; however, their preparation, unlike phthalocyanine formation, is a low-yielding reaction that is unsuitable for polymer network assembly. Instead, rigid spirocyclic linking groups were introduced directly between preformed porphyrin subunits by means of the efficient dioxane-forming reaction between the *meso*-tetrakis(pentafluorophenyl)porphyrin (monomer **B1**; Scheme 2) and the monomer **A1**. Although in this case the linking group is not wholly composed of fused rings, there is significant steric restriction to rotation about the single carbon–carbon bond at the *meso*-positions of the porphyrins to prevent structural relaxation, as demonstrated by the attainment of Network-PIMs of high surface areas (900–1100 $m^2 g^{-1}$).[35]

It is now clear that dioxane formation (i.e., a double aromatic nucleophilic substitution) offers a general reaction for the preparation of Network-PIMs from appropriate hydroxylated aromatic monomers (e.g., **A1**–**A7**) and fluorinated (or chlorinated) aromatic monomers (e.g., **B1**–**B7**), as shown in Scheme 2.[36] For microporosity, at least one of the rigid monomers must contain a "site of contortion", which may be a spirocentre (e.g., **A1** and **B7**), a single covalent bond around which rotation is hindered (e.g., **A5**, **B1** and

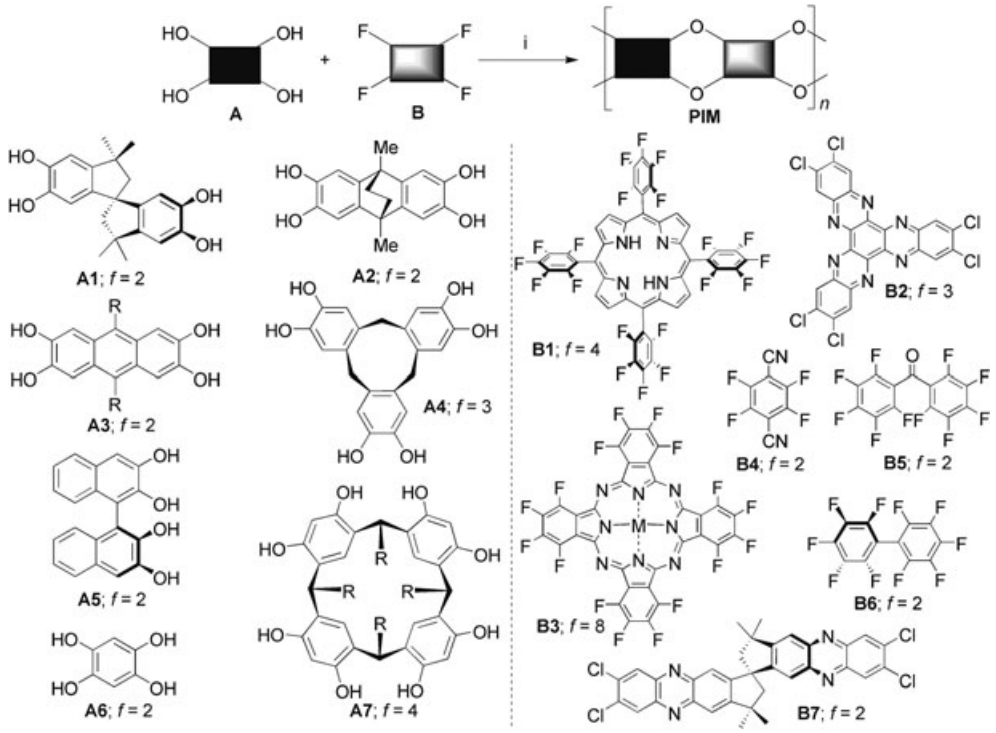

Scheme 2. PIMs are prepared by means of a dioxane-forming polymerisation reaction using a combination of appropriate hydroxylated aromatic monomers (e.g., **A1–A7**) and fluorinated (or chlorinated) aromatic monomers (e.g., **B1–B7**). See text for further details.

B6) or a nonplanar rigid skeleton (e.g., **A2**, **A4** and **A7**). If two planar monomers react together (e.g., **A3** with **B2**), a nonporous material results. To obtain an insoluble network polymer, the average functionality (f_{av}) of the monomer combination should be greater than two ($f_{av} > 2$); for dioxane formation each pair of adjacent hydroxyl groups or fluorines counts as a single functional group. The inexhaustive "pick-and-mix" range of successful monomers includes preformed, fluorinated phthalocyanine **B3**, the tridentate ligand hexachlorohexaazatrinaphthylene **B2** and rigid hydroxylated monomers that possess cavities for hosting organic molecules, such as cyclotricatechylene **A4** or calixresorcarene **A7**.[37]

Creating Microporous Materials Without a Network Structure

All conventional microporous materials (e.g., zeolites and carbons) are network polymers held together by robust covalent bonds (Figure 3a and 3c). Network-PIMs have an amorphous structure similar to activated carbon (Figure 3c). Crystalline zeolites analogues such as the MOFs are effectively networks with strong noncovalent cross-links composed of metal–ligand or multiple hydrogen bonds (Figure 3b); some of these display swelling in the presence of an adsorbate. We wished to answer the question: can intrinsic microporosity be obtained from a polymer without a network structure? The relatively weak intermolecular interac-

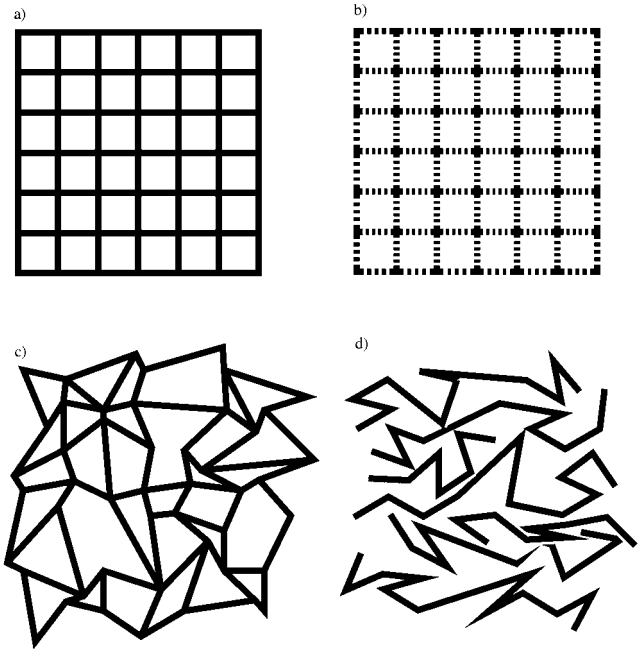

Figure 3. Two-dimensional representations of microporous structures. a) Crystalline ordered material composed of a covalent network (e.g., zeolites). b) Crystalline ordered material composed of strong noncovalent interactions (e.g., MOFs). c) Amorphous covalent network (e.g., activated carbon and network-PIMs). d) A non-network material composed of a rigid and contorted polymer (e.g., PIM-1).

tions within such a material could be reversibly disrupted by solvent to allow solution processing—a clear advantage over other microporous materials.

Generally, polymers pack space efficiently because the macromolecules can bend and twist to maximise intermolecular interactions. However, it has long been recognised that some polymers can possess large amounts of void space, which is usually referred to as free volume. It is reasonable to anticipate that above a certain amount of free volume the voids would be interconnected and, therefore, the polymer will behave as a conventional microporous material despite the lack of a network structure (Figure 3d). A polymer held above its glass transition temperature (T_g) exists in a rubbery state and has a relatively large amount of free volume due to transient voids existing between the highly mobile polymer chains. On cooling below its T_g, the proportion of free volume decreases so that there is insufficient space for large-scale movements of the polymer backbone, and the polymer then behaves as a rigid glass. For most polymers, the fraction of free volume that remains in the glassy state is relatively small, but for some polymers that possess a rigid molecular structure, it is possible to "freeze-in" a larger amount of free volume (up to 20%) by cooling or the rapid removal of a solvent. Such high free-volume glassy polymers (e.g., polyimides, polyphenyleneoxides, etc.) are used in the manufacture of membranes as the voids assist the transport of gas or liquid across the material, but these voids are not interconnected, and the accessible surface area, as measured by gas adsorption, is low. However, there are a few examples of "ultra-high free-volume" polymers, best represented by the much studied polyacetylene derivative poly(1-trimethylsilyl-1-propyne) (PTMSP) and the fluoropolymer Teflon AF 2400 (a copolymer of 4,5-difluoro-2,2-bis(trifluoromethyl)-1,3-dioxole and tetrafluoroethylene).[38] These polymers have been classified as microporous on the basis of exceptionally high gas permeabilities, which can be 2–3 orders of magnitude higher than those displayed by conventional high free-volume polymers, suggesting that their free volume (~30%) is interconnected.[39] Masuda first described PTMSP in 1983[40] and since that time it has been the focus of considerable fundamental and applied interest, especially for membrane applications.[41]

In this context, it was of interest to prepare non-network polymers from various combinations of the bifunctional monomers (Scheme 2; $f_{av}=2$) that had proved successful in forming Network-PIMs. If at least one of the two precursor monomers contains a "site of contortion" (e.g., **A1**, **A2**, **A5** or **B7**), the dioxane-forming polymerisation reaction gives polymers that possess high surface areas as powdered solids (500–850 $m^2 g^{-1}$; Figure 4).[48] These polymers of intrinsic microporosity (PIMs) confirm that a network structure is not

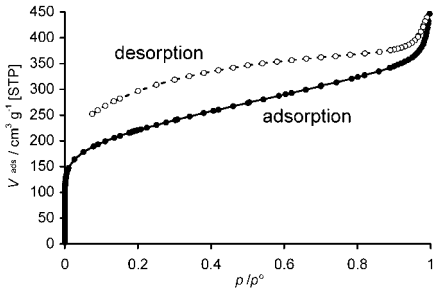

Figure 4. The nitrogen adsorption/desorption isotherm at 77 K for a powdered sample of PIM-1. From the isotherm a BET surface area of 850 $m^2 g^{-1}$ can be calculated. The shape of the isotherm indicates marked hysteresis, which may be related to the ability of the polymer to swell in nonsolvents—in this case condensed nitrogen.

necessary for the generation and maintenance of microporosity within an organic material. Instead, intrinsic microporosity can arise simply from a polymer whose molecular structure is highly rigid and contorted so that space-efficient packing in the solid state is prohibited (Figure 5). In particular, the lack of rotational freedom along the polymer backbone ensures that the macromolecules cannot rearrange

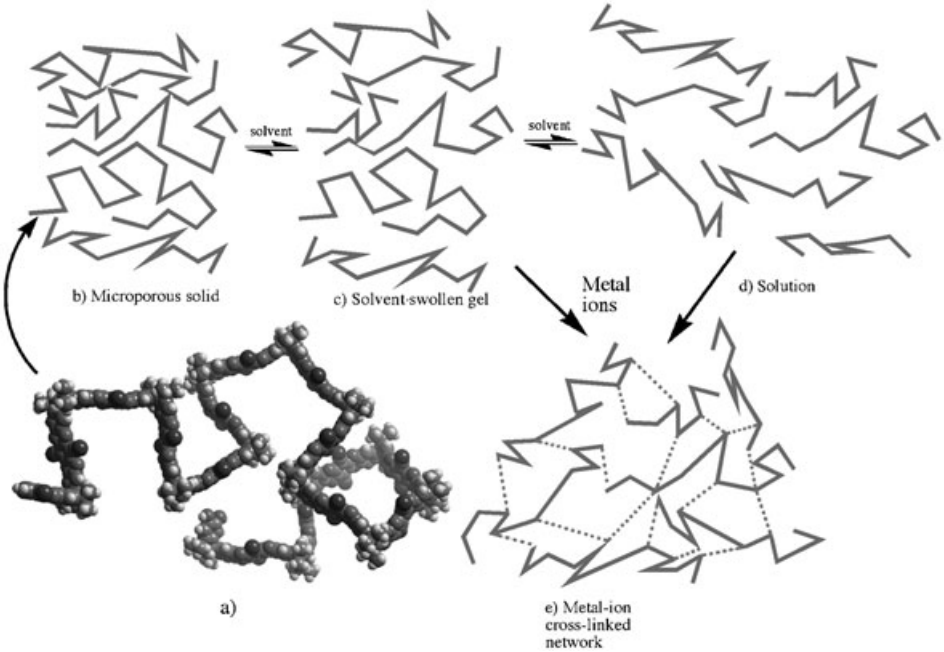

Figure 5. a) Model of a molecular fragment of PIM-1 showing its randomly contorted structure together with cartoon representations of the various states that can be obtained from a PIM including: b) a microporous solid due to the inability of the polymer molecules to pack efficiently, c) a solvent-swollen gel, d) solution and e) a metal-ion cross-linked microporous network.

their conformation to collapse the open structure of the material. Differential scanning calorimetry shows no glass transition or melting point for each of the polymers, and samples of powdered material heated to below their decomposition temperatures (300 °C for 24 h) or left for prolonged periods of time (>1 year) under ambient conditions display similar surface areas to freshly precipitated samples. Thus, so long as the polymer's molecular structure remains intact, its microporosity and mechanical robustness are maintained.[50]

Despite their rigid structures, these PIMs are freely soluble in some organic solvents, which allows an estimation of their average molecular mass by gel-permeation chromatography. The highly fluorescent spiropolymer PIM-1 (Table 1), derived from monomers **A1** and **B4** and consisting of a completely fused-ring structure, proved to be of particularly high molecular mass (typically, $M_w = 140\,000\ g\,mol^{-1}$), which confirms the exceptional efficiency of the dioxane-forming polymerisation reaction. The high molar mass and good solubility of PIM-1 allow conventional solution-based polymer processing techniques to be applied. For example, robust, self-standing films of high optical clarity and high surface area ($650\ m^2\,g^{-1}$) can be prepared by simply casting from solution (Figure 6). Dynamic mechanical thermal analysis of a cast film of PIM-1 shows a tensile storage modulus (E') of about 1 GPa, in the range expected for a glassy polymer; a value that hardly decreases as the temperature is increased up to 350 °C in air (Figure 7).

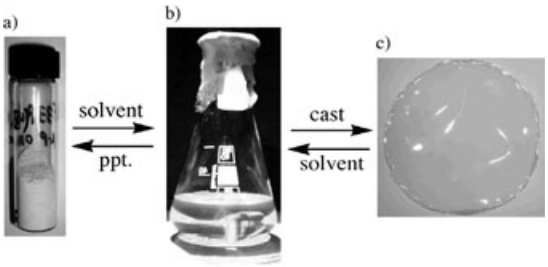

Figure 6. PIM-1 a) in powdered form, b) in THF, and c) as a solvent cast film suitable for use as a membrane.

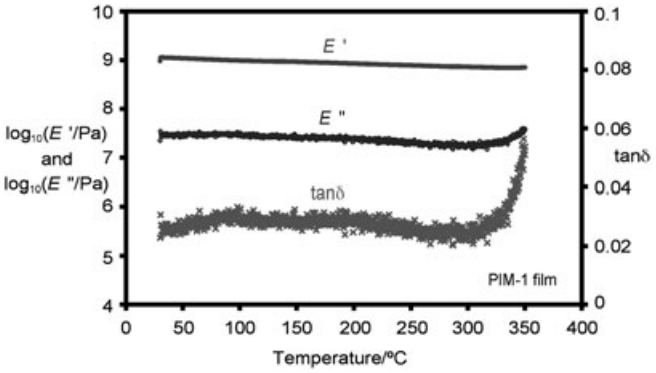

Figure 7. Dynamic mechanical thermal analysis of PIM-1 self-standing film: dependence on temperature of (left-hand axis) tensile storage modulus E' and tensile loss modulus E'' and (right-hand axis) loss tangent, $tan\,\delta$.

Table 1. Gas permeability data for a range of polymers of interest for gas separation membranes.

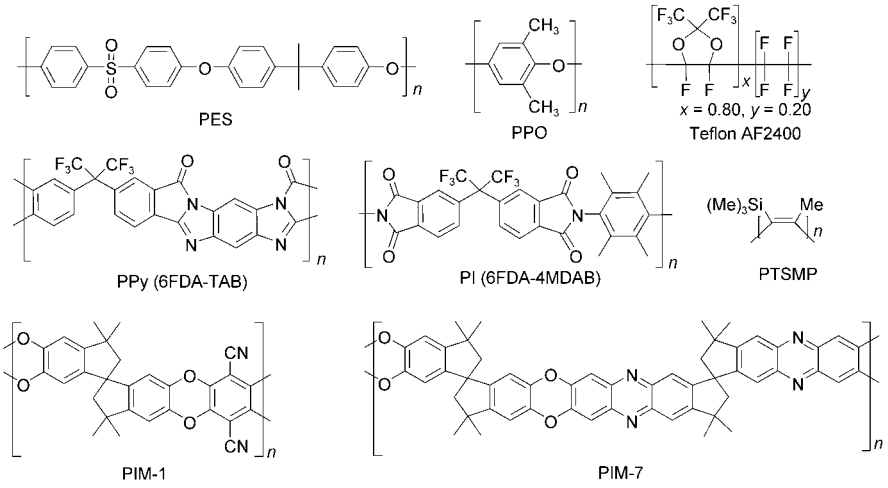

Polymer	T_g [°C]	$P(O_2)$ [Barrer][a]	$\alpha(O_2/N_2)$ [$cm^2\,s^{-1}$]	$D(O_2)\times10^8$ [cm^3(STP)]	$S(O_2)\times10^3$ [$cm^{-3}\,cmHg^{-1}$]	SA[b]	Ref.
PES	185	1.4	5.6	4.4	3.2	[c]	[42]
PPO	207	12	4.6	12	10	[c]	[43]
PPy(6FDA-TAB)	>400	15	5.9	7.0	21	[c]	[44]
Teflon (AF 2400)	250	1140	2.1	850	12	[c]	[38,45]
PI (6FDA-4MDAB)	430	122	3.4	66	19	650	[46a,49]
PTMSP	>200	9000	1.4	5200	15	950	[45,47]
PIM-1	>400	370	4.0	82	46	850	[48,49]
PIM-7	>400	190	4.5	62	30	750	[49]

[a] Barrer = $\times10^{-10}\,cm^3$(STP)$\,cm^{-1}\,s^{-1}\,cmHg^{-1}$; [b] SA = BET surface area of powdered sample. [c] Not measured.

As anticipated, the solution processability of PIMs offers a significant advantage over conventional insoluble microporous materials in, for example, the preparation of membranes or for the application of microporous coatings. These materials are also able to swell reversibly in the presence of a non-solvent such as MeOH (Figure 5c), which may also provide a valuable advantage in applications such as adsorption. We believe that the ability of the polymers to swell may also contribute to the hysteresis observed in their nitrogen adsorption isotherm (e.g., Figure 4). In this case, as nitrogen is condensed within the micropores the structure of the material relaxes allowing access to voids that were inaccessible at lower relative pressures.

Gas Permeability: Evidence for a Continuous Spectrum of Free Volume for Rigid Polymers

The study of the gas permeability of polymers is a well-established technological field due to the extensive commercial interest in using polymer-derived membranes for gas separations. Over the past four decades an enormous volume of data has been compiled on the two main performance indicators of a polymer: the permeability coefficient $P(x)$ for a particular gas (x) and the selectivity of one gas (x) over another (y), which in most cases is ideal selectivity, $\alpha(x/y) = P(x)/P(y)$, derived from single-gas permeability measurements. For a useful polymer membrane it is desirable to have both high permeability and high selectivity. Some preliminary permeability data for PIM-1 and PIM-7 is given in Table 1, along with similar data for a selection of polymers of interest for the fabrication of gas separation membranes. As might be expected for microporous materials, films of PIMs are highly gas permeable with only the "ultra-permeable" polymers, most notably poly(1-trimethylsilyl-1-propyne) (PTMSP) and Teflon AF 2400, demonstrating higher overall gas permeability.

Unfortunately, polymers that give highly selective membranes are generally of low permeability and vice versa. Robeson has quantified this trade-off by developing the idea of an upper bound in double logarithmic plots of selectivity against permeability.[51,52] For example, an updated Robeson plot for O_2 versus N_2 is given in Figure 8, on which data for

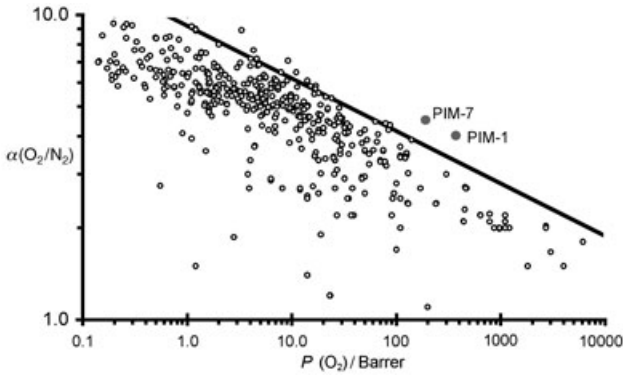

Figure 8. The Robeson plot showing the trade-off between polymer gas permeability and ideal selectivity for oxygen versus nitrogen. The empirical upper bound line is shown and is based upon the polymers that demonstrated the best selectivity for a given permeability in 1991. For commercial separation membranes, it is desirable to obtain polymers whose data points lies above the upper bound line and towards the top right-hand side of the plot.

PIM-1 and PIM-7 are also plotted. Since the original plots were published in 1991, there has been significant development of polymers with high selectivity at low permeability, in addition to the disclosure of further examples of ultra-high free-volume polymers exhibiting very high permeability but low selectivity.[53] However, it has proved difficult to achieve polymers with the desirable combination of high permeability (e.g., oxygen permeability, $P(O_2) > 100$ Barrer) and good selectivity (e.g., $P(O_2)/P(N_2) > 3.5$). Polymers PIM-1 and PIM-7 show substantially higher selectivities than other polymers of similar permeability, and represent a significant advance across Robeson's upper limit. PIMs also lie above or near to the upper bound line for several other commercially important gas combinations, including CO_2/CH_4, H_2/N_2 and H_2/CH_4. This behaviour indicates that these PIMs are inherently different to the many hundreds of polymers that have been investigated for gas permeability, including the microporous ultra-permeable polymers, and it is of interest to speculate as to the cause of this difference.

Gas permeation through polymer membranes is frequently discussed in terms of a simple solution-diffusion model, for which the permeability coefficient (P) is the product of a diffusion coefficient (D) and a solubility coefficient (S). For a glassy polymer, the main factor influencing the diffusion coefficient for a given gas is the amount of free volume within the polymer. The solubility coefficient is related to the strength of the intermolecular interactions between the gas and the polymer. It has been noted[54] that polymers that lie on or close to Robeson's upper bound line all possess very rigid molecular structures. These include polypyrrolones (e.g., 6FDA-TAP)[44] and certain polyimides (e.g., 6FDA-4MDAB)[46] in which rigidity is engineered by the use of trifluoromethyl and methyl substituents to restrict rotation within the polymer backbone. PIM-1 and PIM-7, for which rigidity and the prohibition of rotation are ensured by their rigid spirocyclic fused-ring structures, are possibly the ultimate expression of this design concept.

For O_2 and N_2, the measured values of D and those of S calculated from D and P on the basis of the solution-diffusion model are given in Table 1. The separation achieved by each polymer is dominated by the mobility selectivity, which favours the smaller oxygen molecule (diameter = 0.346 nm) rather than the larger nitrogen molecule (diameter = 0.364 nm) and, for a microporous polymer, is primarily dependent on the size distribution of the micropores. For PIM-1 and PIM-7, the contribution of solubility selectivity in favour of oxygen is small, but the overall values of solubility are extraordinarily high, significantly higher than the values typically encountered with other polymers. Thus, the improved performance of PIMs over Robeson's upper bound line is linked to large apparent solubilities, boosting the permeability whilst maintaining selectivity. The high apparent solubility of gases in PIMs may be attributed in part to their microporous character, which provides a high capacity for gas uptake. Furthermore, the PIMs incorporate polar groups that strengthen intermolecular interactions and encourage sorption. In PIM-1, the nitrile groups may be assumed to enhance both the strength of intermolecular forces and, because of their lateral position, the free volume, giving rise to even higher apparent solubilities than PIM-7. In contrast, for the ultrapermeable polymers such as PTMSP, the high permeability arises largely from very high diffusion coefficients (Table 1). PTMSP, like the PIMs described here, exhibits microporous character in low-temperature N_2 sorption

analysis, but there are differences in the sorption behaviour at very low relative pressures that suggest a larger average, and broader distribution of, apparent pore size for PTMSP as compared to the PIMs (Figure 9). As the pore size increases, different transport mechanisms come into play, such as surface diffusion. Larger pores allow more rapid diffusion, but diminish selectivity for light gases.

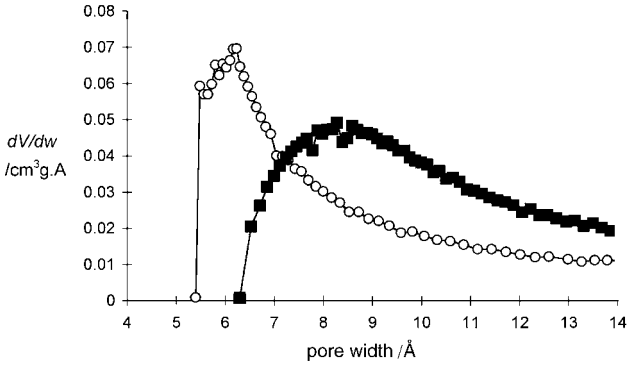

Figure 9. Apparent pore size distributions calculated by Horvath–Kawazoe method (slit pore, carbon-graphite model) for powder samples of PIM-1 (open circle) and freshly precipitated PTMSP (solid square) derived from N_2 adsorption/desorption results.

The concept of enhancing gas–polymer interactions, and hence permeability, of a polymer system by the addition of polar substituents (e.g., nitrile, nitro, etc.) has been dismissed previously, due to the concomitant increase in polymer cohesion energy, which generally reduces free volume and thereby permeability.[55] For PIMs, the highly rigid molecular structure can clearly tolerate strongly polar groups without causing the collapse of free volume suffered by other more flexible polymers. The ability to introduce highly polar functional groups without compromising microporosity is an important feature of the PIMs and will allow the further design of selective polymers for gas separations with even greater permeability.

Potential applications of PIMs

As demonstrated above, the combination of high permeability and good selectivity makes PIMs interesting candidates for gas membrane applications, such as the generation of oxygen-enriched air for enhanced combustion and fermentation processes or for the removal of CO_2 from methane. In this context there is a general demand for ultrapermeable polymers of good thermal and chemical stability, especially as the technological potential of PTMSP (a polymer that has attracted a great deal of attention in the patent literature)[41] is severely limited due to its rapid loss of microporosity on standing and lack of chemical stability towards heat, radiation or UV light in the presence of oxygen.[41,55]

However, gas separation is just one of several areas where PIMs have technological potential. Being organic microporous materials with amorphous structures related to that of activated carbon, it was anticipated that the Network-PIMs should be suitable for the adsorption and separation of organic compounds, and this has been confirmed by measuring the adsorption of phenol from aqueous solution. This process is of environmental relevance as phenols are common contaminants of wastewater streams from industrial processes. The Network-PIM, of surface area $850\,m^2g^{-1}$, derived from the spiromonomer **A1** and hexachlorohexaazatrinaphthylene **B2**, adsorbs up to $5\,mmol\,g^{-1}$ of phenol from solutions of initial concentration of $0.2\,mol\,L^{-1}$ (i.e., 0.5 g of phenol for 1 g of Network-PIM). In addition, this material can be used for the efficient removal of phenol from water at low concentration ($5–20\times10^{-4}\,mol\,L^{-1}$).[36] Similar results are obtained from phthalocyanine-based Network-PIMs. Carbons with comparable specific surface areas exhibit maximum adsorption capacities for phenol in the range 1–4 $mmol\,g^{-1}$ from aqueous solution.[56–59]

The removal of phenol from aqueous solution has also been achieved by pervaporation of robust self-standing films derived from soluble PIM-1 or PIM-7 as membranes.[50] Pervaporation is a process in which the feed is a liquid mixture and a vacuum is applied to the opposite side of the membrane to remove permeate as a vapour, which is then condensed and collected. In Figure 10 it can be seen that, with the PIM-1 membrane, the permeate was enriched in phenol up to tenfold, which demonstrates that the membrane is strongly organophilic (i.e., selective for organic compounds over water).

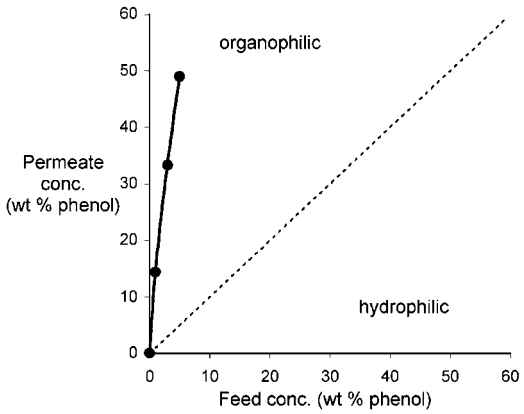

Figure 10. Pervaporation-based separation of phenol from aqueous solution using a membrane derived from PIM-1. Generally, the efficiency of separation may be expressed as a separation factor, $\alpha=(Y_o/Y_w)/(X_o/X_w)$, in which (Y_o/Y_w) is the weight ratio of organic compound to water in the permeate and (X_o/X_w) is the weight ratio of organic compound to water in the feed. Values of α of 16–18 were obtained at temperatures in the range 50–80 °C and feed compositions in the range 1–5 wt % phenol.[50]

For Network-PIMs containing either the phthalocyanine, porphyrin or hexaazatrinaphthylene subunit, it is possible to introduce appropriate transition-metal ions for catalytic activity. Preliminary studies on the degradation of hydrogen peroxide by using metal-containing porphyrin or phthalocyanine networks show a greatly enhanced rate relative to

nonporous microcrystalline model compounds.[37] In addition, the hexaazatrinaphthylene subunit is a well-established ligand capable of forming a complex with up to three transition-metal ions.[60] Exposing the orange network polymer to a solution of bis(benzonitrile)palladium(II) dichloride in chloroform gave a highly coloured material with a mass loading of palladium dichloride of 40%.[36] Nitrogen adsorption analysis of the material subsequent to metal adsorption gave a specific surface area of 347 $m^2 g^{-1}$. Much of the loss of specific surface area can be attributed to the gain in mass (65%) of the material rather than a loss of intrinsic microporosity. Clearly, such Network-PIMs offer great potential as heterogeneous catalysts and chemoselective adsorbents.

Similar metal-containing materials of even higher specific surface area can be derived from PIM-7 by exploiting the ability of its phenazine subunits to act as a ligand for metal-ion coodination. Thus the addition of bis(benzonitrile)palladium(II) dichloride to a yellow solution of PIM-7 causes an immediate precipitation of a red solid that is insoluble in all solvents. This material contains over 20% by mass Pd^{2+} and has a surface area of 650 $m^2 g^{-1}$. It can be deduced that the Pd^{2+} ion acts as a cross-link between the PIM macromolecules to give a network material (Figure 5e). Recent work has shown that these palladium-containing microporous materials successfully act as efficient heterogeneous catalysts for aryl–aryl coupling Suzuki reactions.[37] Of interest is the observation that a solvent cast film of PIM-7, swollen in methanol, can also be cross-linked by Pd^{2+} ions to give an insoluble network (Figure 11). This process has potential for the fabrication of reactive membranes.

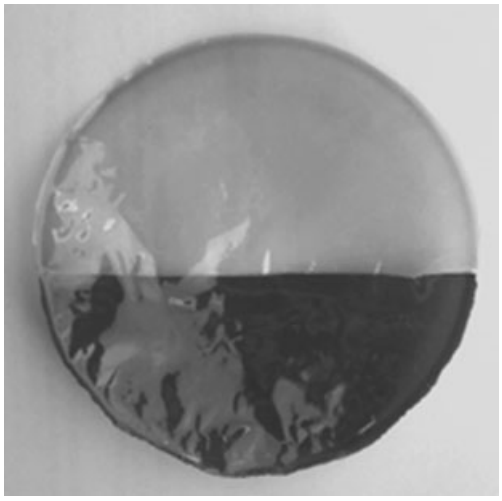

Figure 11. A solvent cast film of PIM-7. The darker portion has been treated with a solution of palladium(II) dichloride bis(benzonitrile) and is no longer soluble in organic solvents, indicating formation of a metal-ion cross-linked network polymer (see Figure 5e).

Conclusion

The area between two established fields of technology is often a stimulating and rewarding research environment. We believe that PIMs effectively bridge the gap between conventional microporous materials and polymers, because they possess properties common to both classes of material. The potential offered by the structural diversity of PIMs, which can be controlled simply by the choice of monomer precursors, remains largely unexplored. Nevertheless, the few examples that have been studied suggest an enticing prospect of readily processed, custom-made organic microporous materials designed to adsorb, or react with, target molecules by using the principles of molecular recognition. It can be assumed that once a potentially useful material is recognised its performance can be tuned incrementally by synthesis. Ultimately, the concept of PIMs may be developed to provide materials to engage in highly specific processes that mimic the sophisticated "lock-and-key" receptor sites found in enzymatic catalysis.[61]

PIMs provide another example of the utility of amorphous organic materials. The fascinating and beautiful crystalline mimics of zeolites that increasingly grace the pages of journals will stimulate welcome interest in organic microporous materials. Ultimately, however, commercial applications may result from materials that can be readily fabricated into useful forms. A lesson to be learned from the development of polymers and organic electronic materials is that it pays to play to the strengths of organic materials (e.g., processability and the exquisite control over structure and function through synthesis). The PIMs concept is built upon the firm foundations of polymer technology and we believe that it offers a highly practical approach to organic microporous materials.

Acknowledgements

The authors wish to thank EPSRC, DSTL, the IAC and Kuwait University for funding.

[1] In *Handbook of Porous Solids*, *Vol. 1–5* (Eds.: F. Schüth, K. Sing, J. Weitkamp), Wiley-VCH, Berlin, **2002**.
[2] M. E. Davis, *Nature* **2002**, *417*, 817–821.
[3] T. J. Barton, L. M. Bull, W. G. Klemperer, D. A. Loy, B. McEnaney, M. Misono, P. A. Monson, G. Pez, G. W. Scherer, J. C. Vartuli, O. M. Yaghi, *Chem. Mater.* **1999**, *11*, 2633–2656.
[4] F. Schüth, W. Schmidt, *Adv. Mater.* **2002**, *14*, 629–638.
[5] S. Kitagawa, R. Kitaura, S.-I. Noro, *Angew. Chem.* **2004**, *116*, 2388–2430; *Angew. Chem. Int. Ed.* **2004**, *43*, 2334–2375.
[6] O. M. Yaghi, M. O'Keefe, N. W. Ockwig, H. K. Chae, M. Eddaoudi, J. Kim, *Nature* **2003**, *423*, 705–714.
[7] M. Eddaoudi, J. Kim, N. Rosi, D. Vodak, J. Wachter, M. O'Keefe, O. M. Yaghi, *Science* **2002**, *295*, 469–472.
[8] M. Simard, D. Su, J. D. Wuest, *J. Am. Chem. Soc.* **1991**, *113*, 4696–4698.
[9] Y. Diskin-Posner, S. Dahal, I. Goldberg, *Angew. Chem.* **2000**, *112*, 1344–1348; *Angew. Chem. Int. Ed.* **2000**, *39*, 1288–1292.
[10] M. E. Kosal, J.-H. Chou, S. R. Wilson, K. S. Suslick, *Nat. Mater.* **2002**, *1*, 119–121.
[11] M. E. Kosal, K. S. Suslick, *J. Solid State Chem.* **2000**, *152*, 87–98.
[12] D. W. Smithenry, S. R. Wilson, K. S. Suslick, *Inorg. Chem.* **2003**, *42*, 7719–7721.
[13] P. Brunet, T. Maris, M. Simard, J. D. Wuest, *J. Am. Chem. Soc.* **1997**, *119*, 2737–2738.

[14] X. Wang, T. Maris, M. Simard, J. D. Wuest, *J. Am. Chem. Soc.* **1994**, *116*, 12119–12120.
[15] T. Tanaka, T. Tasaki, Y. Aoyama, *J. Am. Chem. Soc.* **2002**, *124*, 12453–12462.
[16] J. W. Patrick, in *Porosity in Carbons* (Ed.: J. W. Patrick), Edward Arnold, London, **1995**.
[17] K. Kaneko, C. Ishii, M. Ruike, H. Kuwabara, *Carbon* **1992**, *30*, 1075–1088.
[18] L. R. Radovic, in *Chemistry and Physics of Carbon: A Series of Advances*, *Vol. 27* (Ed.: L. R. Radovic), Marcel Dekker, New York, **2001**, p. 227.
[19] D. Lennon, D. T. Lundie, S. D. Jackson, G. J. Kelly, S. F. Parker, *Langmuir* **2002**, *18*, 4667–4673.
[20] C. L. Mangun, Z. Yue, J. Economy, S. Maloney, P. Kemme, D. Cropek, *Chem. Mater.* **2001**, *13*, 2356–2360.
[21] M. Kruk, M. Jaroniec, K. P. Gadkaree, *J. Colloid Interface Sci.* **1997**, *192*, 250–256.
[22] Y. Aoyama, *Top. Curr. Chem.* **1998**, *198*, 131–161.
[23] T. Sawaki, Y. Aoyama, *J. Am. Chem. Soc.* **1999**, *121*, 4793–4798.
[24] T. Sawaki, T. Dewa, Y. Aoyama, *J. Am. Chem. Soc.* **1998**, *120*, 8539–8540.
[25] P. Battioni, E. Cardin, M. Louloudi, B. Schöllhorn, G. A. Spyroulias, D. Mansay, T. G. Traylor, *Chem. Commun.* **1996**, 2037–2038.
[26] F. Karpowicz, J. Hearn, M. C. Wilkinson, *Adsorption* **2000**, *6*, 337–347.
[27] N. R. Cameron, D. C. Sherrington, *Adv. Polym. Sci.* **1996**, *126*, 163.
[28] B. Sellergren, K. J. Shea, *J. Chromatogr.* **1993**, *635*, 31–49.
[29] O. W. Webster, F. P. Gentry, R. D. Farlee, B. E. Smart, *Makromol. Chem. Macromol. Symp.* **1992**, *54/55*, 477.
[30] C. Urban, E. F. McCord, O. W. Webster, L. Abrams, H. W. Long, H. Gaede, P. Tang, A. Pines, *Chem. Mater.* **1995**, *7*, 1325–1332.
[31] N. B. McKeown, *Phthalocyanine Materials: Synthesis, Structure and Function*, Cambridge University Press, Cambridge, **1998**.
[32] N. B. McKeown, *J. Mater. Chem.* **2000**, *10*, 1979–1995.
[33] N. B. McKeown, S. Makhseed, P. M. Budd, *Chem. Commun.* **2002**, 2780–2781.
[34] B. Meunier, *Chem. Rev.* **1992**, *92*, 1411.
[35] N. B. McKeown, S. Hanif, K. Msayib, C. E. Tattershall, P. M. Budd, *Chem. Commun.* **2002**, 2782–2783.
[36] P. M. Budd, B. Ghanem, K. Msayib, N. B. McKeown, C. Tattershall, *J. Mater. Chem.* **2003**, *13*, 2721–2726.
[37] P. M. Budd, B. S. Ghanem, H. Kingston, S. Makhseed, N. B. McKeown, K. Msayib, C. E. Tattershall, unpublished results.
[38] A. Yu, Y. Yampolskii, V. P. Shantarovich, S. M. Nemser, N. A. Plate, *J. Membr. Sci.* **1997**, *126*, 123–132.
[39] R. Srinivasan, S. R. Auvil, P. M. Burban, *J. Membr. Sci.* **1994**, *86*, 67–86.
[40] T. Masuda, E. Isobe, T. Higashimura, K. Takada, *J. Am. Chem. Soc.* **1983**, *105*, 7473–7475.
[41] K. Nagai, T. Masuda, T. Nakagawa, B. D. Freeman, I. Pinnau, *Prog. Polym. Sci.* **2001**, *26*, 721–795.
[42] J. S. McHattie, W. J. Koros, D. R. Paul, *Polymer* **1991**, *52*, 844–850.
[43] A. Y. Alentiev, E. Drioli, M. Gokzhaev, G. Golemme, O. M. Ilinitch, A. A. Lapkin, V. Volkov, Y. Yampolskii, *J. Membr. Sci.* **1998**, *138*, 99–107.
[44] C. M. Zimmerman, W. J. Koros, *J. Polym. Sci. Part B* **1999**, *37*, 1235–1249.
[45] A. Yu, V. Shantarovich, T. C. Merkel, V. I. Bondar, B. D. Freeman, Y. Yampolskii, *Macromolecules* **2002**, *35*, 9513–9522.
[46] a) K. Tanaka, M. Okano, H. Toshino, H. Kita, K.-I. Okamoto, *J. Polym. Sci. Part B* **1992**, *30*, 907–914; b) M. Al-Masri, H. R. Kricheldorf, D. Fritsch, *Macromolecules* **1999**, *32*, 7853–7858.
[47] Y. Yampolskii, A. P. Korikov, V. Shantarovich, K. Nagai, B. D. Freeman, T. Masuda, M. Teraguchi, G. Kwak, *Macromolecules* **2001**, *34*, 1788–1796.
[48] P. M. Budd, B. S. Ghanem, S. Makhseed, N. B. McKeown, K. Msayib, C. E. Tattershall, *Chem. Commun.* **2004**, 230–231.
[49] D. Fritsch, N. B. McKeown, P. M. Budd, K. J. Msayib, presented at the *Second Advanced Membrane Technology Conference*, Kloster Irsee (Germany), **2004**, and at *Euromembrane 2004*, Hamburg (Germany), **2004**..
[50] P. M. Budd, E. S. Elabas, B. S. Ghanem, S. Makhseed, N. B. McKeown, K. Msayib, C. E. Tattershall, D. Wang, *Adv. Mater.* **2004**, *16*, 456–459.
[51] L. M. Robeson, *J. Membr. Sci.* **1991**, *62*, 165–186.
[52] L. M. Robeson, W. F. Burgoyne, M. Langsam, A. C. Savoca, C. F. Tien, *Polymer* **1994**, *35*, 4970–4978.
[53] A. Y. Alentiev, Y. P. Yampolskii, *J. Membr. Sci.* **2000**, *165*, 201–216.
[54] B. D. Freeman, *Macromolecules* **1999**, *32*, 375–380.
[55] R. E. Kesting, A. K. Fritzsche, *Polymeric Gas Separation Membranes*, Wiley-Interscience, New York, **1993**.
[56] H. S. Teng, S. C. Wang, *Carbon* **2000**, *38*, 817–824.
[57] B. Okolo, C. Park, M. A. Keane, *J. Colloid Interface Sci.* **2000**, *226*, 308–317.
[58] C. Moreno-Castilla, J. Rivera-Utrilla, M. V. López-Ramón, F. Carrasco-Marín, *Carbon* **1995**, *33*, 845–851.
[59] X. Liu, N. G. Pinto, *Carbon* **1997**, *35*, 1387–1397.
[60] V. J. Catalano, W. E. Larson, M. M. Olmstead, H. B. Gray, *Inorg. Chem.* **1994**, *33*, 4502–4509.
[61] J. M. Lehn, *Supramolecular Chemistry*, VCH, Weinheim, **1995**.

Published online: January 13, 2005